restricted extracellular space, or accumulation inside the fiber, cannot be responsible for inactivation of the inward current. Depletion, or accumulation, would depend on current size, not on the ion species.

The slowing of inactivation in both $Sr^{2+}$ and $Ba^{2+}$ Ringer was accompanied by a marked prolongation of action potentials in these solutions (*17*), emphasizing that the kinetics of the Ca channel are influenced by the permeant ion. We also found a similar, though much less marked, effect on the activation kinetics of the channel: inward currents turned on faster (Fig. 2, A and B) and the inward current tails turned off faster (*18*) in $Ca^{2+}$ than they did in $Ba^{2+}$.

Our experiments show that steady-state inactivation of the Ca permeability has a voltage dependence similar to that of the inward current and that the rate of inactivation is, at least partly, dependent on the permeant ion. This is in marked contrast to the Na channel of nerve fibers, where the species of the permeant ion does not significantly affect the kinetics of activation and inactivation. Our findings suggest that inactivation of the Ca permeability in insect muscle, as in *Paramecium* and *Aplysia* neurons, is caused by an interaction of the permeant ion with the channel, the ion having to traverse the membrane to produce inactivation. We do not know whether permeant ions bind to a site at the inner membrane surface to produce inactivation or if they influence inactivation during their passage through the membrane by interaction with a site in the Ca channel.

FRANCES M. ASHCROFT*
P. R. STANFIELD
*Department of Physiology,*
*University of Leicester,*
*Leicester LE1 7RH, United Kingdom*

### References and Notes

1. S. Hagiwara and L. Byerly, *Annu. Rev. Neurosci.* **4**, 69 (1981).
2. S. Hagiwara *et al.*, *J. Physiol. (London)* **219**, 233 (1971); J. Hildalgo, M. Luxoro, E. Rojas, *ibid.* **288**, 313 (1979).
3. B. Katz and R. Miledi, *ibid.* **203**, 459 (1969); P. F. Baker and T. J. Rink, *ibid.* **253**, 593 (1975).
4. R. W. Meech and N. B. Standen, *ibid.* **249**, 211 (1975).
5. R. D. Keynes, E. Rojas, R. E. Taylor, J. Vergara, *ibid.* **229**, 409 (1973).
6. J. A. Connor, *ibid.* **286**, 41 (1979).
7. S. Hagiwara, S. Ozawa, O. Sand, *J. Gen. Physiol.* **65**, 617 (1975).
8. A. L. Hodgkin and A. F. Huxley, *J. Physiol. (London)*, **116**, 497 (1952).
9. P. Brehm and R. Eckert, *Science* **202**, 1203 (1978).
10. D. Tillotson, *Proc. Natl. Acad. Sci. U.S.A.* **76**, 1497 (1979).
11. F. M. Ashcroft, N. B. Standen, P. R. Stanfield, *J. Physiol. (London)* **291**, 51 (1979).
12. The apparent reversal potential refers to the potential at which the membrane current reverses in sign and is considerably more negative than the Ca equilibrium potential ($E_{Ca}$) because of contamination by leakage and residual outward currents.
13. H. Meves, *Prog. Biophys. Mol. Biol.* **33**, 207 (1978).
14. W. Almers, R. Fink, P. T. Palade, *J. Physiol. (London)* **312**, 177 (1981).
15. $E_K$ was raised to around −50 mV in these experiments by increasing $[K]_o$ to 40 m*M* because of the rapid decay of the current tails at more negative potentials. In this Ringer, $[K]_i$ measured with intracellular K-selective microelectrodes (ion-exchange resin, Corning 477317) had a mean value of 297.9 ± 3.9 m*M* (111 fibers, eight muscles) at 20°C, giving an $E_K$ of −50.3 ± 0.3 mV.
16. Peak inward current in Ca Ringer was −112.5 ± 14.4 μA cm$^{-2}$ ($N$ = 14) and −96.05 ± 13.2 μA cm$^{-2}$ ($N$ = 6) in Sr Ringer.
17. Mean action potential duration in $Ca^{2+}$ was 0.35 ± 0.05 second ($N$ = nine fibers), 4.1 ± 0.4 seconds ($N$ = 11) in $Sr^{2+}$, and 147 ± 58.1 seconds ($N$ = 6) in $Ba^{2+}$.
18. Decay of inward current tails followed a single exponential with a time constant of 2.64 msec in Ca Ringer and of 5.55 msec in Ba Ringer at −40 mV.
19. R. H. Adrian, W. K. Chandler, A. L. Hodgkin, *J. Physiol. (London)* **208**, 607 (1970).
20. The peak Sr and Ba, but not Ca, currents during pulse 2 were smaller than the current at the end of pulse 1 (see Fig. 2, A and B). This does not imply that inactivation continues during the interval in $Ba^{2+}$ and $Sr^{2+}$ solutions. Hodgkin-Huxley theory [A. L. Hodgkin and A. F. Huxley, *J. Physiol. (London)* **117**, 500 (1952)] predicts that if inactivation does not fully recover during the interval, then by the time the inward current has reached its peak during pulse 2, inactivation may have declined to a lower level than at the end of pulse 1. The pulse 2 current will therefore be smaller. The effect may not be apparent in $Ca^{2+}$ solution because both activation and recovery from inactivation are faster than in solutions of $Ba^{2+}$ or $Sr^{2+}$.
21. We thank H. E. Edwards for a gift of K-selective resin and N. B. Standen for reading the manuscript. The intercellular [K] measurements were made by C. A. Leech, whom we thank, in collaboration with F.M.A. The work was supported by the Medical Research Council.
* Present address: Department of Physiology, University of California, Los Angeles 90024.

3 September 1980; revised 8 April 1981

## Three Distinct Genes in Human DNA Related to the Transforming Genes of Mammalian Sarcoma Retroviruses

Abstract. *Southern blot hybridization was used to identify human and other vertebrate DNA sequences that were homologous to cloned DNA fragments containing the oncogenic nucleic acid sequences of three different type C mammalian retroviruses (simian sarcoma virus, the Snyder-Theilen strain of feline sarcoma virus, and the Harvey strain of murine sarcoma virus). Each* onc *gene counterpart has a single genetic locus, which probably contains non-*onc *intervening sequences. The human DNA sequences may represent genes important to cell growth or cell differentiation, or both. Their identification and isolation may allow elucidation of their role in these processes and in neoplasias.*

All rapidly transforming retroviruses contain nucleotide sequences specific for transformation (termed *onc* genes) and linked to portions of a helper leukemia virus genome (*1*). The *onc* genes are homologous to subsets of normal host cellular DNA that are well conserved among vertebrates (*1*). The cellular homologs of *onc* genes may play a role in neoplastic transformation. Tumor induction in chickens by the avian leukosis virus (RAV-2) is associated with downstream promotion of a cellular gene (*c-myc*) related to the transforming gene of avian myelocytomatosis virus MC29 (*2, 3*). A similar cellular gene present in two diverse species, the chicken and the cat, was found in the genomes of the Fujinami avian sarcoma virus and two strains of feline sarcoma virus (Snyder-Theilen and Gardner-Arnstein) (*4*). All three of the *onc* gene products have associated protein kinase activity (*5, 6*). The number of cellular genes that could be transduced by retroviruses is probably limited, and it is likely that related genes in diverse species have similar functions and may have a role in cell transformation. It is therefore important to determine whether similar genes are present in humans and to analyze these genes before examining their role in cell growth, differentiation, and tumorigenesis in man.

We used molecularly cloned DNA fragments containing transformation-specific sequences of three mammalian sarcoma retroviruses—the woolly monkey (simian) sarcoma virus (SSV), the Snyder-Theilen strain of feline sarcoma virus ($FeSV_{ST}$), and the Harvey murine sarcoma virus (HaMSV)—to detect homologous DNA sequences in man and lower vertebrates by Southern (*7*) hybridization. These viruses differ from each other in their hosts of origin (primate, cat, and rat, respectively), in the arrangement of their genes, and in the structure of the *onc*-specific protein. Like a number of other acutely transforming retroviruses including Abelson murine leukemia virus (*8*) and the avian viruses MC29 (*9*), avian erythroblastosis virus (*10*), and Fujinami sarcoma virus (*11*), $FeSV_{ST}$ codes for a fused polypeptide containing *gag*- and *onc*-directed peptides and an associated tyrosine protein kinase activity (*12, 13*). The gene order of $FeSV_{ST}$ is 5′-*gag-onc-env-C*-3′ (*gag* and *env* are antigenic determinants of core and envelope proteins, respectively, and *C* is a noncoding region) (*14*). The HaMSV is a double recombinant containing the 5′ and 3′ termini of the


0036-8075/81/0710-0226$00.50/0 

Moloney strain of murine leukemia virus (Moloney-MuLV) [0.1 and 0.9 kilobases (kb), respectively] and approximately 0.9 kb of transforming sequences near the 5′ end; the rest (3.0 kb) is homologous to endogenous 30*S* rat RNA (*15, 16*). The transforming protein of HaMSV is a 21,000-dalton molecule that exhibits guanosine diphosphate–binding activity (*17*). The genetic structure of SSV was elucidated when molecular clones of SSV and its helper simian sarcoma–associated virus (SSAV) were obtained (*18*). Heteroduplex and restriction enzyme mapping has shown that the SSV 6.3-kb genome has an *onc*-specific sequence of about 1.2 kb and that the gene order for SSV is 5′-*gag-env-onc-C*-3′, which is similar to that of Moloney-MSV (*19, 20*). The *onc*-specific sequences of SSV are unrelated to other viral *onc* genes (*21*). The gene product of SSV *onc* has not been unambiguously identified, but cloned SSV DNA selected messenger RNA from SSV-transformed nonproducer cells that synthesized a 20,000-dalton protein in vitro (*22*). These three mammalian sarcoma viruses thus represent three different types of structures of rapidly transforming retrovirus genomes.

The probes used in this study were (i) the intact SSV genome linked to Charon 21A arms, (ii) two pBR322 recombinant plasmids, which together contained approximately 1.2 kilobase pairs (kbp) of the 1.4-kbp transforming region of $FeSV_{ST}$ (*23*), and (iii) a pBR322 plasmid with a 6.6-kbp HaMSV insert (*24*). These recombinant DNA molecules were labeled in vitro by nick translation (*25*).

All three probes detected bands in human, subhuman primate, and chicken DNA (Fig. 1). Samples of DNA from chimp, human, gibbon, woolly monkey, dog, and chicken were digested with Bam HI and hybridized to the SSV probe (Fig. 1A). Two fragments (approximately 8.6 and 1.9 kbp) were found in DNA from all four primates. One band of 4.3 kbp was detected in chicken DNA and three bands of 7.3, 3.9, and 2.1 kbp were detected in dog DNA. Materials on duplicate filters hybridized to cloned SSAV DNA labeled with $^{32}P$ showed no detectable bands (data not shown). The intensity of the bands detected by SSV are similar to those in DNA from all the species. This suggests a strong conservation of the homologous sequences from chicken to man.

The *onc* gene of FeSV was derived from cat cellular DNA (*26*). Direct comparison of the restriction maps of viral and cellular *onc* elements showed that most, if not all, of the restriction endonuclease sites are conserved between the two and that, in addition, the cellular *onc* sequences are interrupted by at least three stretches of noncoding sequences (*23*). Specific DNA fragments were detected in Sac I–digested DNA from human, baboon, dog, and chicken (Fig. 1B). The FeSV probe recognized three Sac I fragments in human, baboon, and dog DNA and one fragment in chicken DNA. Two of the three Sac I fragments are conserved between human and baboon DNA.

The HaMSV probe detected two Kpn I fragments (7.6 and 4.1 kbp) in human DNA and one Kpn I fragment in baboon (4.9 kbp) and chicken (13.7 kbp) DNA (Fig. 1C). Again, the similar intensity of the bands in the three DNA samples suggests a high degree of conservation of HaMSV sequences among the different vertebrate species.

Human DNA was digested with different restriction enzymes and hybridized to the three mammalian sarcoma virus probes. In our limited survey of different primary normal and neoplastic tissues as well as tissue culture cell lines, we did not detect any polymorphism of the *onc* gene loci. When used with the SSV probe, Eco RI cleaved human DNA to yield a single fragment of 23 kbp (Fig. 2). This result suggests that there is a single locus for SSV-related DNA sequences. Digestion with Bam HI showed at least one site within the SSV-related *onc* gene that generated two dominant bands, while digestion with Xba I revealed three bands of 30.0, 9.8, and 3.9 kbp. Since these patterns were reproducible even after the amount of enzyme was increased fivefold, they were probably not the results of incomplete digestion. The size of the SSV-specific sequences is only 1.2 kbp, which is smaller than that

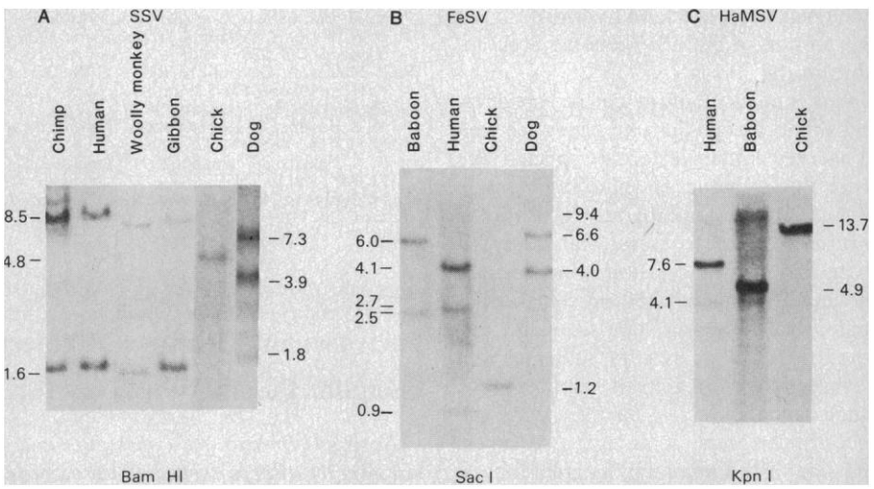


Fig. 1. Conservation of cellular *onc* genes related to SSV, FeSV, and HaMSV. Total cellular DNA (20 μg) from different species, as indicated, was digested with 60 units of restriction endonucleases (Bam HI, Sac I, or Kpn I) for 20 hours; the fragments were separated by electrophoresis on a 0.8 percent agarose gel. The DNA was transferred to nitrocellulose filters (*7*) and hybridized to $^{32}P$-labeled probes (~ $2 \times 10^6$ count/min) prepared by nick translation (*25*) of cloned DNA (specific activity ~ $2 \times 10^8$ cpm/μg). Molecular weights are given in kilobase pairs.

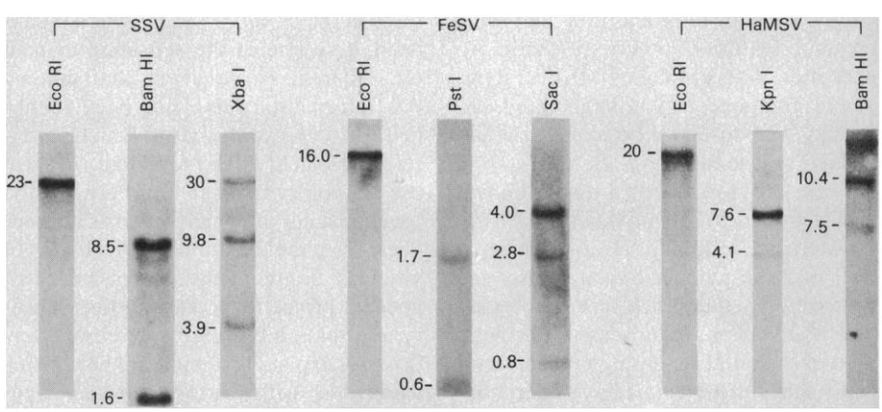


Fig. 2. Restriction patterns of the human *onc* genes related to SSV, FeSV, and HaMSV. Human DNA (normal placenta) was digested with the specified restriction endonucleases and hybridized to $^{32}P$-labeled SSV, FeSV, and HaMSV probes as described in the legend to Fig. 1.

of any of the three fragments generated by Xba I; thus the SSV-related *onc* gene in humans is probably interrupted by noncoding sequences.

The FeSV *onc*-specific probe also detected a single locus in human DNA digested with Eco RI (Fig. 2). The size of this fragment (16 kbp) is different from the one detected by SSV. Two and three bands, respectively, were produced by Pst I and Sac I (Fig. 2). The sum of the sizes of these fragments is again greater than that of the *onc* sequences.

The HaMSV probe hybridized to one Hind III fragment and two Kpn I and Bam HI fragments of human DNA (Fig. 2). Although HaMSV contains, in addition to the *onc* gene, sequences homologous to rat 30*S* RNA, the endogenous virus-like 30*S* RNA sequences would be expected to be less well conserved phylogenetically than the *onc* sequences. However, we cannot rule out the possibility that a subset of the bands detected in human DNA is due to hybridization of the portion of HaMSV genome homologous to the 30*S* RNA.

Our studies confirm earlier observations that the cellular *onc* genes are well conserved among vertebrate species. We were able to detect specific fragments in human DNA homologous to sarcoma viruses isolated from cat, rat, and primate, using hybridization conditions of moderate stringency (50 percent formamide; triple-strength standard saline citrate; 60°C). Our results indicate that each cellular *onc* gene is confined to a single genetic locus, distinct from the loci of the others. In at least two cases, the size of the *onc* locus is greater than that of the viral *onc* specific sequences, suggesting the presence of intervening sequences not related to *onc*. This is borne out by direct cloning of the human cellular homologs of the FeSV- and SSV-related *onc* genes (*27*). The presence of introns has been reported in cellular *onc* genes of Abelson-MuLV (mouse) (*28*) and FeSV (cat) (*23*), and they may be a common feature of other *onc* genes. An exception is the Moloney-MSV system, where complete and uninterrupted homology was observed between viral and cellular *onc* sequences (*29*).

There are now about a dozen known viral *onc* genes. All of them may have counterparts in human DNA. The presence of these genes in humans raises the question whether they are expressed constitutively or are turned on specifically in certain differentiating or neoplastic cells. Since these genes have been conveniently parceled into retroviruses, they can be used as probes to answer these questions.

*Note added in proof*: In surveying a large number of human DNA samples, we have found more than one allelic forms of the *onc* loci of SSV and HaMSV (*30*).

FLOSSIE WONG-STAAL
RICCARDO DALLA-FAVERA
GENOVEFFA FRANCHINI
EDWARD P. GELMANN
ROBERT C. GALLO

*Laboratory of Tumor Cell Biology, National Cancer Institute, National Institutes of Health, Bethesda, Maryland 20205*

### References and Notes

1. P. H. Duesberg, *Cold Spring Harbor Symp. Quant. Biol.* **14**, 13 (1980).
2. B. G. Neel, W. S. Hayward, H. L. Robinson, J. Fang, S. M. Astrin, *Cell* **23**, 323 (1981).
3. W. S. Hayward, B. G. Neel, S. M. Astrin, *Nature (London)* **290**, 475 (1981).
4. M. Shibuya, T. Hanafusa, H. Hanafusa, J. R. Stephenson, *Proc. Natl. Acad. Sci. U.S.A.* **77**, 6536 (1980).
5. W. J. M. Van de Ven, F. W. Reynolds, J. R. Stephenson, *Virology* **101**, 185 (1980).
6. M. Barbacid, K. Beemon, S. G. Devare, *Proc. Natl. Acad. Sci. U.S.A.* **77**, 5158 (1980).
7. E. M. Southern, *J. Mol. Biol.* **98**, 503 (1975).
8. O. N. Witte, A. Dasgupta, D. Baltimore, *Nature (London)* **283**, 826 (1980).
9. P. Mellon, A. Dawson, K. Bister, G. S. Martin, P. H. Duesberg, *Proc. Natl. Acad. Sci. U.S.A.* **75**, 5874 (1978).
10. M. J. Hayman, B. Royer-Pokora, T. Graf, *Virology* **92**, 31 (1979).
11. R. A. Feldman, T. Hanafusa, H. Hanafusa, *Cell* **22**, 757 (1980).
12. M. Barbacid, A. V. Lauver, S. G. Devare, *J. Virol.* **33**, 196 (1980).
13. S. K. Ruscetti, L. P. Turek, C. J. Sherr, *ibid.* **35**, 259 (1980).
14. C. J. Sherr, L. A. Fedele, L. Donner, L. P. Turek, *ibid.* **32**, 860 (1979).
15. Y. H. Chien, M. Lai, T. Y. Shih, I. M. Verma, E. M. Scolnick, P. Roy-Burman, N. Davidson, *ibid.* **31**, 752 (1979).
16. R. W. Ellis, D. Defeo, J. M. Maryak, H. A. Young, T. Y. Shih, E. H. Chang, D. R. Lowry, E. M. Scolnick, *ibid.* **36**, 408 (1980).
17. T. Y. Shih, M. O. Weeks, H. A. Young, E. M. Scolnick, *Virology* **96**, 64 (1979).
18. E. P. Gelmann, F. Wong-Staal, R. Kramer, R. C. Gallo, *Proc. Natl. Acad. Sci. U.S.A.*, in press.
19. D. J. Donoghue, P. A. Sharp, R. A. Weinberg, *J. Virol.* **32**, 1015 (1979).
20. C. J. Sherr, L. A. Fedele, M. Oskarsson, J. Maizel, G. F. Vande Woude, *ibid.* **34**, 200 (1980).
21. F. Wong-Staal, E. P. Gelmann, R. Dalla-Favera, S. Szala, S. Josephs, R. C. Gallo, unpublished data.
22. ———, V. Manzari, unpublished data.
23. G. Franchini, J. Even, C. J. Sherr, F. Wong-Staal, *Nature (London)* **290**, 154 (1981).
24. G. L. Hager *et al.*, *J. Virol.* **31**, 795 (1979).
25. P. N. Rigby, M. Dieckmann, C. Rhodes, P. Berg, *J. Mol. Biol.* **113**, 236 (1977).
26. A. E. Frankel, J. H. Gilbert, K. J. Porzig, E. M. Scolnick, S. A. Aaronson, *J. Virol.* **30**, 821 (1979).
27. R. Dalla-Favera, E. P. Gelmann, R. C. Gallo, F. Wong-Staal, *Nature (London)*, in press; G. Franchini, F. Wong-Staal, R. Dalla-Favera, R. C. Gallo, unpublished data.
28. S. P. Goff, E. Gilboa, O. N. Witte, D. Baltimore, *Cell* **22**, 777 (1980).
29. M. Oskarsson, W. L. McClements, D. G. Blair, J. V. Maizel, G. F. Vande Woude, *Science* **207**, 1222 (1980).
30. F. Wong-Staal, R. Dalla-Favera, G. Franchini, E. P. Gelmann, R. C. Gallo, E. Westin, S. Arya, unpublished results.
31. We thank M. Martin for the gift of cloned HaMSV plasmid DNA and C. Sherr for FeSV recombinant phage from which subclones of the *onc* region were constructed.

2 February 1981; revised 14 April 1981

## Perivascular Meningeal Projections from Cat Trigeminal Ganglia: Possible Pathway for Vascular Headaches in Man

Abstract. *Peroxidase-containing cell bodies were found in the ipsilateral trigeminal ganglia after horseradish peroxidase was applied to the proximal segment of the middle cerebral artery in seven cats. Cell bodies containing the enzyme marker were located among clusters of cells that project via the first division. The existence of sensory pathways surrounding large cerebral arteries provides an important neuroanatomical explanation for the hemicranial distribution of headaches associated with certain strokes and migraine.*

The proximal segments of large cerebral arteries are among the few structures in the cranium which, when stimulated, give rise to the sensation of pain (*1*). Afferent nerve fibers that convey this information have not been identified. However, the areas to which pain is referred (such as the forehead) suggest the possibility of a relation between the trigeminal nerve, which receives afferent fibers from the cranium, and head pain of vascular origin. Thus perivascular trigeminal projections, transmitting sensory information from large cerebral arteries, may explain the unilateral head pains associated with certain vascular syndromes such as strokes, classical migraine, and cluster headaches (*2*).

We have initiated neuroanatomical studies to determine uptake and transport of horseradish peroxidase (HRP) (*3*) by neurons surrounding the middle cerebral artery to cell bodies in the trigeminal ganglia. Our results indicate that, in the cat, sensory afferents surround the proximal segment of the middle cerebral artery and project ipsilaterally from cell bodies in the first division of the trigeminal ganglia. Should such first-order afferent fibers exist in man (*1*), this would provide an explanation for the distribution of hemicranial vascular headaches.

Using microsurgical techniques and a dissecting microscope (magnification, ×25), we applied HRP to the right middle cerebral artery in seven cats (2 to 4 kg) (*4*). To restrict the diffusion of HRP away from the artery, HRP (3 mg) was


0036-8075/81/0710-0228S00.50/0 